Hydrogeophysical Approach for Identification of Layered Structures of the Vadose Zone from Electrical Resistivity Data

Alexandre M. Tartakovsky,* Diogo Bolster, and Daniel M. Tartakovsky

The electric resistivity survey and borehole collection of resistivity data are one of the oldest geophysical tools for characterization of the vadose zone. A current trend is to conduct such surveys in a tomographic manner, which requires significant computational resources. We present a simple, semianalytical approach to delineate multiple layers in partially saturated soils from resistivity and saturation measurements taken at several depths along a borehole. The number of layers and their hydraulic properties are assumed to be known. The proposed inversion algorithm is computationally efficient and can serve either as a stand-alone tool for layer delineation or as an autonomous module in a more comprehensive geophysical survey. It is most robust when each layer is sampled at least once. When one or more layers have not been sampled, the algorithm's robustness (convergence) depends on the accuracy of an initial guess (e.g., expert knowledge and other hard or soft data). We provide a detailed analysis of the algorithm's convergence and identify potential pitfalls.

H ETEROGENEITY and lack of sufficient site characterization render accurate and reliable predictions of subsurface flow and transport in the vadose zone notoriously elusive. It is now widely recognized that for quantitative descriptions of subsurface phenomena to be scientifically defensible, they have to be accompanied by some measure of predictive uncertainty. In other words, a major goal of subsurface modeling is to translate uncertainty about soil properties (e.g., hydraulic conductivity and dispersivity) and driving forces (e.g., infiltration rates and the location and amount of a spill) into uncertainty about system states (e.g., soil moisture and contaminant concentration) (Tartakovsky and Winter, 2008). This task can be accomplished by treating soil properties and other input parameters as random fields whose statistics are inferred from available data; the resulting flow and transport equations become stochastic (e.g., Rubin, 2003, and references therein).

A.M. Tartakovsky, Pacific Northwest National Lab., Richland, WA 99352; D. Bolster, Technical Univ. of Catalonia, Barcelona, Spain; D.M. Tartakovsky, Dep. of Mechanical and Aerospace Engineering, Univ. of California-San Diego, La Jolla, CA 92093. Received 15 Jan. 2008. *Corresponding author (Alexandre.Tartakovsky@pnl.gov).

In general, solving these equations either analytically or numerically requires a closure approximation, which limits the applicability of such solutions. For example, perturbation closures of stochastic unsaturated flow equations (e.g., Tartakovsky and Guadagnini, 2001; Tartakovsky et al., 2003), which are often used in stochastic hydrology, are based on the assumption that a subsurface environment is only mildly heterogeneous. Two-point closures, also known as Corrsin's conjecture, (e.g., Neuman, 1993) and four-point closures (Dentz and Tartakovsky, 2008) of stochastic transport equations impose distributional assumptions (e.g., stationarity and Gaussianity) on the advective velocity, which might or might not hold true. The random domain decomposition (Winter and Tartakovsky, 2000, 2002; Winter et al., 2002) provides a general framework that enables one to overcome these limitations by explicitly accounting for both the geologic structure of a subsurface environment and the uncertainty associated with its delineation.

The approach relies on a tacit assumption that available data allow reconstruction (albeit probabilistically) of major geologic units, e.g., layers comprising the vadose zone. This task can be accomplished by geostatistical (e.g., Ritzi et al., 1994; Guadagnini et al., 2004) or other (e.g., Wohlberg et al., 2006; Tartakovsky et al., 2007) analyses of material properties data, including hydraulic conductivity and soil texture, etc.—the so-called forward facies delineation problem. Such data are hard to come by and expensive to collect. They often have to be supplemented with measurements of hydraulic system states (e.g., soil moisture and pressure head) or their geophysical counterparts (e.g., electrical resistivity or permittivity), giving rise to the so-called inverse

facies delineation problem. Recent advances in the use of geophysics for subsurface imaging, such as ground penetrating radars, time domain reflectometry, microwave radiometry, and downhole electromagnetic induction, were the subjects of the November 2004 special issue of the *Vadose Zone Journal* on hydrogeophysics (Vereecken et al., 2004).

Electric resistivity surveys, one of the oldest geophysical tools for subsurface characterization, have been regaining popularity in recent years for a variety of reasons, some of which were discussed by Dahlin (1996) and Cornacchiulo and Bagtzoglou (2004). Chief among them are advances in inverse modeling of geophysical data (e.g., Hubbard and Rubin, 2000; Yeh et al., 2002; Michalak and Kitanidis, 2003; Cornacchiulo and Bagtzoglou, 2004; Furman et al., 2004) that are accompanied and facilitated by advances in computing power. The latter is essential since these and other inversion approaches are computationally demanding. This is especially so for electrical resistivity surveys of the multilayered vadose zone, where electrical resistivity varies with saturation. Despite significant advances in inverse modeling and data fusion (see Liu and Yeh, 2004, and the references therein), the absence of analytical or semianalytical solutions to inverse modeling translates into the absence of benchmark problems on which the accuracy and robustness of numerical inversion and data assimilation codes can be tested.

We have developed a semianalytical inversion procedure that allows interpretations of electrical resistivity data to be conditioned on a solution of the Richards equation. The inverse approach can be used—either as a stand-alone tool or as a component of a tomographic procedure (e.g., Griffiths and Barker, 1993; Storz et al., 2000)—to delineate boundaries between soil layers from electric resistivity and hydraulic data. The former can be collected at various depths with borehole measurements (e.g., Spies, 1996; Binley et al., 2002), while the latter can be obtained by analyzing soil samples assumed to represent homogeneous soil layers. This goal is distinct from previous studies of borehole electric surveys. For example, a lot of attention has been paid to the analysis of electrical fields in layered, fully saturated subsurface environments (e.g., Mundry and Zschau, 1983; Sato and Sampaio, 1980; Sato, 2000) or to the monitoring of moisture redistribution (e.g., Binley et al., 2002) and contaminant transport (e.g., Kemna et al., 2002) in layered soils whose spatial extent and hydraulic properties are known.

Theory

Consider a set of M resistivity measurements $\hat{r}_m = r(z_m)$ that are collected in a borehole at depths z_m ($m = 1, \ldots, M$) in the layered vadose zone. Let us assume that the number, N, of layers and their hydraulic properties (but not their location) are either known from a core analysis or can be ascertained by other means, including expert knowledge. No restrictions are placed on the measurement locations; they might or might not sample all the layers. Our goal is to identify the locations of $N-1$ interfaces between these N layers.

Since no tomographic procedure is implied, and since resistivity r is strongly influenced by variable saturation θ, such data alone are not sufficient to accomplish this task. Additional information can be gained by using a phenomenological model to relate r and θ. We used Archie's law:

$$r(z) = \rho_i \left[\theta(z)\right]^{-n_i}$$
$$\rho_i = r_w \phi_i^{-m_i} \qquad \text{for } i = 1, \ldots, N \qquad [1]$$
$$z_{i-1} \le z < z_i$$

where ρ_i is the electrical resistivity of the ith layer, r_w is the electrical resistivity of water, and ϕ_i, m_i, and n_i are the porosity, cementation exponent, and saturation exponent of the ith layer, respectively. We assume that these parameters are known for each layer.

The final piece of information is provided by specifying an equation describing the distribution of saturation in a layered soil, supplemented with boundary (and, if necessary, initial) conditions. To simplify the presentation, we assume steady-state flow that can be adequately described by the one-dimensional Richards equation:

$$\frac{d}{dz}\left[K\left(z,\psi\right)\frac{d\left(\psi+z\right)}{dz}\right] = 0, \quad 0 < z < L \qquad [2]$$

where L is the column length, and the unsaturated hydraulic conductivity $K(z,\psi)$ and the pressure head ψ are related to each other and to θ via the Gardner–Russo exponential model:

$$K = K_s \exp\left(\alpha\psi\right)$$
$$\theta = \theta_s \exp\left(\alpha\psi\right) \qquad [3]$$

The saturated hydraulic conductivity K_s, complete saturation θ_s, and the Gardner parameter α (the reciprocal of the macroscopic capillary length scale) vary betweens layers. We assume that these parameters are known and constant within each layer.

This problem formulation is clearly a simplification and serves as a starting point for future generalizations, in which one or more of the assumptions made above will be relaxed. Some of the approaches to achieve this are discussed below.

Moisture Profile

Consider the saturation-based form of the Richards equation (Eq. [2]):

$$\frac{d}{dz}\left[K\left(z,\theta\right)\frac{d\psi}{d\theta}\frac{d\theta}{dz}\right] + \frac{dK\left(z,\theta\right)}{dz} = 0, \quad 0 < z < L \qquad [4]$$

subject to the boundary conditions

$$\theta(0) = \Theta_0 \text{ and } \left(K\frac{d\psi}{d\theta}\frac{d\theta}{dz}\right)_{z=L} = -q \qquad [5]$$

where q is the infiltration rate and Θ_0 is the saturation at $z = 0$. For the constitutive relationships of Eq. [3], a solution of Eq. [4–5] in a uniform medium can be written as

$$\theta = \Theta_0 e^{-\alpha z} + \frac{q}{K_s}\left(e^{-\alpha z} - 1\right) \qquad [6]$$

This solution can be used to determine a moisture distribution in the layered soil depicted in Fig. 1 as follows. In each layer $\Omega_i = [z_{i-1}, z_i]$, $i = 1, \ldots, N$, the saturation is given by
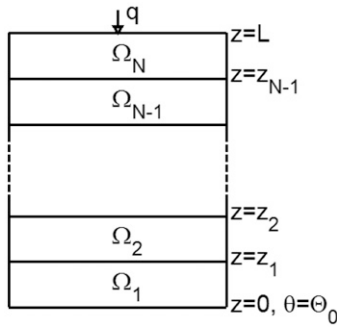
FIG. 1. Layered medium consisting of N homogeneous layers Ω; q is the infiltration rate, L is the column length, z is depth, and $\theta = \Theta_0$ is saturation at $z = 0$.

$$\theta = \Theta_i^{\mathrm{b}}\, e^{-\alpha_i(z-z_i)} + \frac{q}{K_{si}}\left[e^{-\alpha_i(z-z_i)} - 1\right]$$

$$z \in \Omega_i = [z_{i-1}, z_i] \tag{7}$$

where Θ_i^{b} is the (yet unknown) saturation at the bottom of each layer (i.e., at $z = z_{i-1}$).

To determine the values of Θ_i^{b} ($i = 1, \ldots, N$), we note that ψ is continuous across the interfaces between any two adjacent layers, while θ undergoes a corresponding jump whose magnitude depends on the constitutive relation used. For the Gardner–Russo relationships (Eq. [3]), the continuity of pressure yields

$$\Theta_i^{\mathrm{b}} = \left(\Theta_{i-1}^{\mathrm{t}}\right)^{\alpha_i/(\alpha_{i-1})}, \quad i = 1, \ldots, N \tag{8}$$

where Θ_i^{t} is the saturation at the top of the ith layer and, without the loss of generality, we set $\theta_s = 1$ in all layers.

Inverse Procedure

For a given set of hydraulic and electric properties $\{K_{si}, \alpha_i\}_{i=1}^N$ and $\{n_i, m_i\}_{i=1}^N$, the saturation and resistivity profiles are uniquely defined by Eq. [7–8] and [1], respectively. The unknown locations of the interfaces between the layers $\{z_i\}_{i=1}^N$ can now be found by minimizing the objective function J, which is the difference between the computed $r_m = r(z_m)$ and measured $\hat{r}_m$ resistivity values at depths z_m ($m = 1, \ldots, M$):

$$J\left(z_1, z_2, \ldots, z_N\right) = \sum_{m=1}^{M}\left(\hat{r}_m - r_m\right)^2 \tag{9}$$

Solving this N-dimensional optimization problem is not trivial. We found that popular gradient-based optimization methods failed to converge to a global minimum in all but a few special cases. This is probably due to the fact that the solution for saturation in a layered medium is discontinuous at the interfaces. Such discontinuous solutions are known to cause problems for gradient-based optimization schemes.

This finding caused us to settle on the Nelder–Mead algorithm (Nelder and Mead, 1965). This gradient-free optimization method is based on a simplex. In N dimensions, a simplex is a polytope with $N + 1$ vertices (e.g., a line, a triangle, and a tetrahedron in one, two, and three dimensions, respectively). The algorithm consists of the following steps:

1. Generate a simplex using an initial guess.
2. Calculate the values of the objective function at each vertex.
3. Replace the vertex corresponding to the largest value of the objective function with a new point whose selection involves four basic stages: reflect, expand, contract, and shrink (see below).
4. Repeat Steps 2 and 3 until a convergence criterion is satisfied.

During the *reflect* stage, the worst point is reflected through the centroid of the line connecting the two best vertices. If the new point provides a better estimate of the objective function than any of the previous points, we *expand* the search along the line connecting the worst point and this new point, looking for lower values of the objective function. If the new vertex provides a better estimate than the reflected point but not better than the other vertices, we *contract* the search along the line connecting the worst point and this new point. If neither the expansion nor the contraction stage provides a better point, we *shrink* the simplex toward the minimum vertex by projecting all other vertices linearly toward this point with some prespecified multiplier. The algorithm is said to converge once the size of the simplex falls below some prespecified tolerance. For further details on this algorithm, see Nelder and Mead (1965), Lagarias et al. (1998), and the references therein.

The *fminsearch* function in the optimization toolbox in Matlab (The MathWorks, Natick, MA) provides the implementation of the Nelder–Mead algorithm used in the subsequent simulations. One of the downfalls of the Nelder–Mead algorithm is that it can get stuck at small local minima and the original search conditions in *fminsearch* were sufficiently restrictive for this to occur regularly. To avoid this, any time convergence to a minimum occurred without providing a sufficiently small objective function (subject to a specified tolerance), we modified *fminsearch* to reset the search by initially dramatically expanding the size of the simplex to search for lower points. If this expanded search did not work, a new search with a modified initial condition was initiated. Additionally, since for all the problems presented here the convergence was generally rapid (on the order of seconds), we also wrote a code that searched for minima starting from multiple initial conditions scattered uniformly across our search space so as to identify multiple local as well as global minima. We discuss the details of this below.

The ability of the Nelder–Mead algorithm (and other optimization strategies) to converge to a global minimum depends on the accuracy of an initial guess. In our context, an initial guess can be obtained from soft data and expert knowledge (e.g., from a geologic site characterization).

Computational Examples

The following computational examples demonstrate the ability of the proposed inverse procedure to delineate boundaries between layers, its robustness, and potential pitfalls. We start by considering various hydraulic conditions in a two-layer system, and then proceed by exploring several examples in a multilayered system.

Two-Layer System

In the examples below, we consider a soil column of length $L = 10$ m, consisting of two layers, and set the infiltration rate to $q = 2 \times 10^{-3}$ m d^{-1}.

Case 1: Saturation in each layer decreases monotonically with height

This means that within each layer there are no two points that have the same saturation. This regime is achieved by choosing the following parameters: Layer 1: K_{s1} = 1 m d^{-1}, α_1 = 2 m^{-1}, ρ_1 = 12 Ω m, and n_1 = 1.2; Layer 2: K_{s2} = 10 m d^{-1}, α_2 = 1 m^{-1}, ρ_2 = 9 Ω m, and n_2 = 1.7; by setting the interface between the two layers at z_1 = 6 m; and by fixing the saturation at the column's bottom at Θ_0 = 1. The resulting saturation and resistivity profiles are shown in Fig. 2.

In this case, at least one measurement point in the upper layer is needed to recover the interface z_1 = 6 m. This is because, given the particular properties of each layer, a unique value for saturation in the upper layer is guaranteed. On the other hand, if all measurement points are in the lower layer, the convergence to the correct solution cannot be guaranteed. This is because the bottom-layer profiles are the same (up to the initial guess of the interface) regardless of the height of the interface, being governed by both the constant boundary condition at z = 0 and the properties of the bottom layer. The upper layer saturation, however, is sensitive to the interface location, as it determines the interfacial saturation.

Table 1 illustrates this effect by presenting the interface reconstructed from two measurement points for various initial guesses. The inverse procedure correctly reconstructs the interface if the two measurements are taken either in both layers (Case 1a) or only in the upper layer (Case 1c); it fails to converge (i.e., to identify the interface correctly) if both measurements are in the bottom layer (Case 1b). The algorithm's convergence for Case 1a is faster than that for Case 1c. To ensure the convergence in Case 1c, the search parameters for the Nelder–Mead algorithm have to be sufficiently large and the solution bounds have to be enforced. The latter is required to eliminate possible unphysical solutions that predict the interface's position at z_1 < 0 or z_1 > 0.

Case 2: Saturation is uniform throughout most of the upper layer

Saturation is equal to its asymptotic value of θ = q/K_{s2}. (This complicates determination of the interface position, as the value of saturation for each measurement point is not unique.) This regime is achieved by setting α_2 = 4 m^{-1} and placing the interface
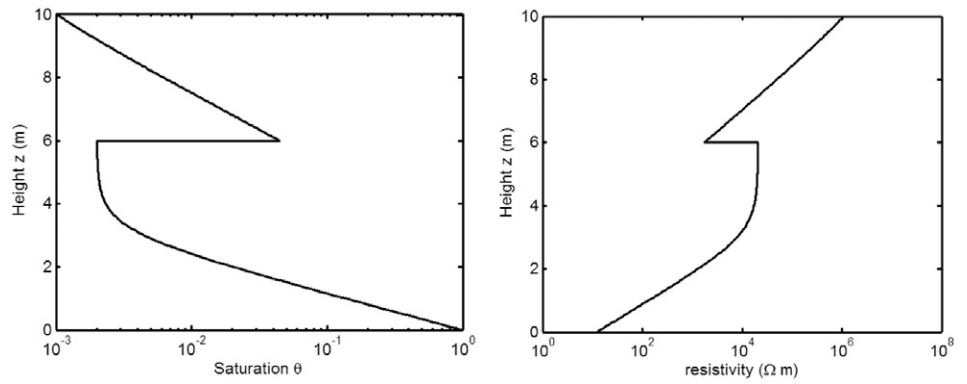

FIG. 2. Saturation (left) and resistivity (right) profiles for Case 1 in the two-layer system.

TABLE 1. Reconstruction of the interface position z_1 = 6 m for initial guesses of 1, 2, 3, …, 8, and 9 m. The two data points used in these reconstructions are located at 2 and 7 m (Case 1a), 2 and 4 m (Case 1b), or 7 and 8 m (Case 1c).

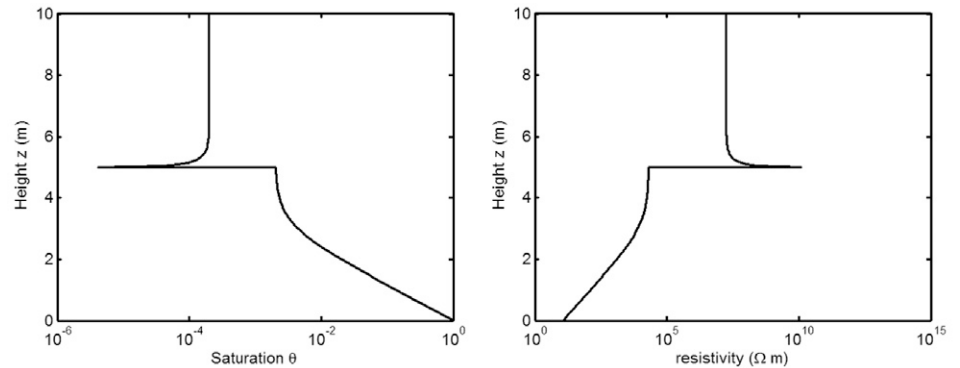| Prediction case	Initial guess of interface position								
	1 m	2 m	3 m	4 m	5 m	6 m	7 m	8 m	9 m
					m				
1a, z_1 =	6	6	6	6	6	6	6	6	6
1b, z_1 =	uc†	uc	uc	4.02	5	6	7	8	9
1c, z_1 =	6	6	6	6	6	6	6	6	6

† uc = unconvergent.

FIG. 3. Saturation (left) and resistivity (right) profiles for Case 2 in the two-layer system.

TABLE 2. Reconstruction of the interface position z_1 = 5 m for initial guesses of 1, 2, 3, …, 8, and 9 m. The two data points used in these reconstructions are located at 2 and 8 m (Case 2a), or 2 and 4 m (Case 2b), or 6 and 8 m (Case 2c).

Prediction case	Initial guess of interface position								
	1 m	2 m	3 m	4 m	5 m	6 m	7 m	8 m	9 m
					m				
2a, z_1 =	5	5	5	5	5	5	5	8.8	9
2b, z_1 =	6–10	6–10	6–10	5	5	6	7	8	9
2c, z_1 =	5	5	5	5	5	5	5	8.7	9

at z_1 = 5 m while keeping the rest of the parameters the same as in Case 1. The resulting saturation and resistivity profiles are shown in Fig. 3.

While Table 2 contains many cases of the correct identification of the interface position, it also provides examples where the inverse algorithm failed to locate the interface. Similar to Case 1, this is particularly true for the case where both measurement points are in the bottom layer (Case 2b). In all cases, if the initial

guess is deep within the upper layer, the solution does not converge to the correct value. This is because, in this case, the saturation in the upper layer quickly reaches it asymptotic value, which makes it virtually impossible to identify the upper layer. In Case 2c, when the initial guess falls within the bottom layer, the predicted interface height varies depending on the specific search parameters used by the optimization algorithm. As long as the initial guess is good (i.e., close to the actual value), however, the result always converges to the correct value.

Case 3: Saturation is uniform throughout most of the bottom layer

Saturation is equal to its asymptotic value of $\theta = q/K_{s1}$. (This complicates determination of the interfacial location, as the value of saturation for each measurement point is not unique.) This regime is achieved by choosing the following parameters: Layer 1: $K_{s1} = 5$ m d^{-1}, $\alpha_1 = 5$ m^{-1}, $\rho_1 = 8$ Ω m, and $n_1 = -1.3$; Layer 2: $K_{s2} = 0.2$ m d^{-1}, $\alpha_2 = 1$ m^{-1}, $\rho_2 = 11$ Ω m, and $n_2 = -1.5$; by setting the interface between the two layers at $z_1 = 5.5$ m; and by fixing the saturation at the column's bottom at $\Theta_0 = 1 \times 10^{-3}$. The resulting saturation and resistivity profiles are shown in Fig. 4.

Table 3 summarizes the results of successful and failed identification of the interface position depending on the measurement locations. Similar to the previous cases, if both measurement points are in the lower layer (Case 3b), it is impossible to guarantee convergence to a single correct value. If an initial guess falls within the bottom part of the lower layer, multiple solutions are obtained depending on the parameters of the optimization algorithm. In the two remaining cases, however, where at least one measurement is taken in the upper layer (Cases 3a and 3c), the interface location is predicted perfectly. Once again, this is because the saturation in the upper layer is very sensitive to saturations at the interface and interface height, and incorrect interfacial heights lead to vertically shifted saturation curves, which do not agree with the experimental values.

Multiple-Layer System

We next apply the proposed algorithm for inversion of electrical resistivity data to soils comprised of multiple homogeneous layers. To be concrete, we present results for a soil column consisting of four layers (Fig. 1 with $N = 4$) and briefly describe reconstruction results for soils consisting of up to eight layers.

In the examples considered below, the length of a soil column is set to $L = 20$ m, with the interfaces between the four layers
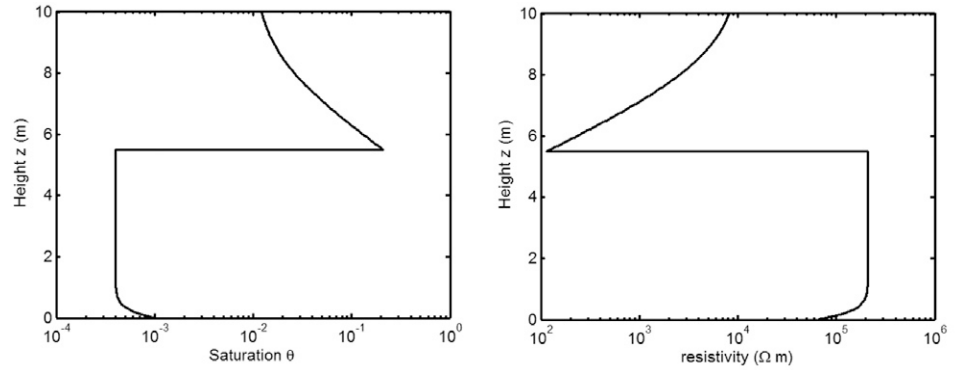

FIG. 4. Saturation (left) and resistivity (right) profiles for Case 3 in the two-layer system.

TABLE 3. Reconstruction of the interface position $z_1 = 5.5$ m for initial guesses of 1, 2, 3, ..., 8, and 9 m. The two data points used in these reconstructions are located at 2 and 8 m (Case 3a), 2 and 4 m (Case 3b), or 6 and 8 m (Case 3c).

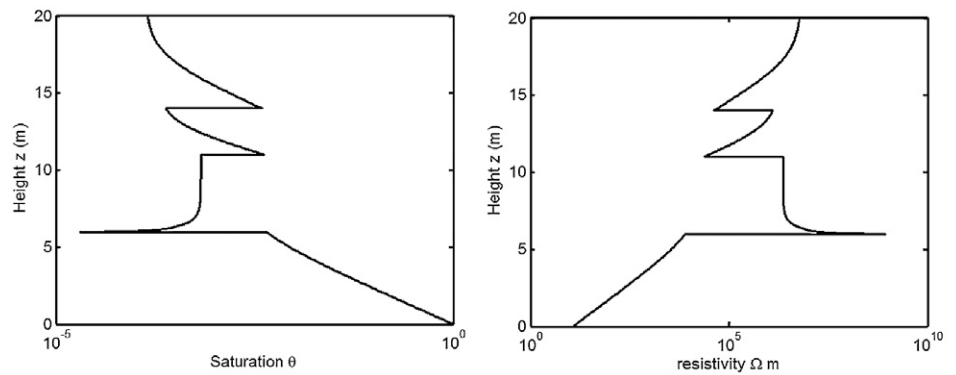| Prediction case	Initial guess of interface position								
	1 m	2 m	3 m	4 m	5 m	6 m	7 m	8 m	9 m
					m				
3a, $z_1 =$	5.5	5.5	5.5	5.5	5.5	5.5	5.5	5.5	5.5
3b, $z_1 =$	1–10	1–10	1–10	4	5	6	7	8	9
3c, $z_1 =$	5.5	5.5	5.5	5.5	5.5	5.5	5.5	5.5	5.5

FIG. 5. Saturation (left) and resistivity (right) profiles for the four-layer system.

located at $z_1 = 6$ m, $z_2 = 11$ m, and $z_3 = 14$ m. The hydraulic and resistivity properties of the four layers are $\alpha = 1, 2, 1.5$, and 1 m^{-1}, $K_s = 1, 3, 10$, and 15 m d^{-1}, $\rho = 12, 9, 11$, and 10 Ω m, and $n = -1.2, -1.7, -1.4$, and -1.5, respectively. The infiltration rate is set to $q = 2 \times 10^{-3}$ m d^{-1} and the saturation at $z = 0$ is set to $\Theta_0 = 1$. The resulting saturation and resistivity profiles are shown in Fig. 5.

Case a: Measurements within each layer

As in the two-layer cases, the availability of measurements from each of the four layers renders the accurate interface reconstruction feasible. It requires a reasonable initial guess, however, especially if a rapid convergence of the optimization algorithm is desired. Otherwise, the optimization algorithm might converge to a local, rather than global, minimum. This is illustrated in Table 4 for the case where our initial guess is 1, 5, and 10 m. If a good initial guess is not available, an iterative algorithm can be written that finds an objective function less than a specified tolerance by expanding the search area of the algorithm. If the initial guess does not converge to a sufficiently small value for the

objective function (in this case it should converge to a value very close to 0), an expanded search begins until the solution converges to the desired value.

Case b: Measurements in several but not all layers

As in the two-layer case, the absence of measurements in every layer leads to decreased fidelity of the reconstruction procedure. The first example in Table 5 shows that even a reasonable initial guess does not guarantee an accurate reconstruction. In this example, four measurements are taken at heights 6.5, 9, 18, and 19 m, i.e., two measurements are in Layer 2 and two in Layer 4. The predicted interface positions are not correct, despite the fact that the objective function is minimized to a value of 0. This indicates the existence of multiple global minima for the objective function. An improved initial guess (the second example in Table 5) leads to convergence to the correct reconstruction. This demonstrates the need to either refine the search algorithm or collect more data or both.

Figure 6 illustrates a range of global minima for which the objective function is zero or close to zero ($<10^{-5}$). This suggests that each of these predicted interface locations would yield the saturations and electrical resistivities that are close to the obtained measurements, thus making it very difficult to tell which of the predictions is actually correct. One can see that the interface between the first two layers is always predicted correctly at 6 m. This is because this interface location is necessary to reproduce the measurements at 6.5 and 9 m. The upper two interfaces, however, are not always accurately captured (although the predictions do appear to fluctuate around the correct values). The interface at 11 m has quite a large range of predicted values (ranging from 9–12 m), while the 14-m interface has a smaller prediction range (13–14.13 m).

The saturation–resistivity profiles corresponding to different interface reconstructions may allow one to distinguish between them. Figure 7 compares the two predictions in Table 5. One can see that the resistivity values at the measurement locations are the same for both cases (in fact they are the same across a large range of the space). There is a large variety of other locations (ranging from 9–14 m), however, where this is not the case. This allows a sampling strategy to be guided by identifying locations where taking measurements would have the highest impact on the reconstruction of the vadose zone. Additional measurements, taken after the initial reconstruction effort, can be used to refine predictions in a manner consistent with Bayesian updating.

Discussion and Conclusions

The electrical resistivity of porous media is a complex function of a medium's properties and water saturation. We have presented a semianalytical inverse approach that allows interpretations of electrical resistivity data to be conditioned on a solution of the Richards equation. The inverse approach was used to delineate interfaces between homogeneous layers in partially saturated

TABLE 4. Reconstruction of the interface positions z_1 = 6, 11, and 14 m for accurate and inaccurate initial guesses. The four data points used in these reconstructions are located at 4, 10, 12, and 17 m.

Initial guess			Predicted values			Objective function
z_1 = 6 m	z_1 = 11 m	z_1 = 14 m	z_1 = 6 m	z_1 = 11 m	z_1 = 14 m	
m						
4	8	16	6	11	14	0
Without expanded search						
1	5	10	1.89	2.6	14.13	2.62×10^{12}
With expanded search						
1	5	10	6	11	14	0

TABLE 5. Reconstruction of the interface positions z_1 = 6, 11, and 14 m for accurate and inaccurate initial guesses. The four data points used in these reconstructions are located in the second (z = 6.5 and 9 m) and fourth (z = 18 and 19 m) layers.

Initial guess			Predicted values			Objective function
z_1 = 6 m	z_1 = 11 m	z_1 = 14 m	z_1 = 6 m	z_1 = 11 m	z_1 = 14 m	
m						
4	8	16	6	9.02	14.13	0
5.8	10.6	14.4	6	11	14	0
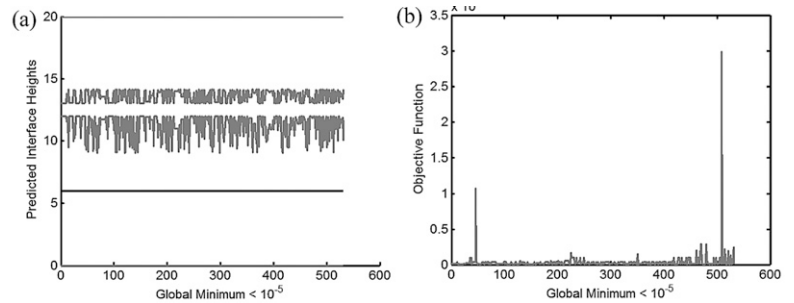
FIG. 6. (a) Predicted interface locations corresponding to the values of objective functions $<10^{-5}$, and (b) the value of the associated objective function.
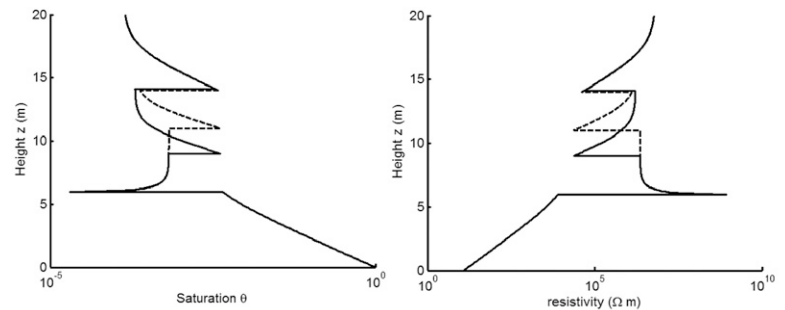

FIG. 7. Saturation (left) and resistivity (right) profiles corresponding to the two interface reconstructions shown in Table 5. The solid line is the correctly predicted value; the dashed line is the incorrect one.

soils from moisture profiles and borehole electrical resistivity data. Our analysis leads to the following major conclusions:

1. The proposed algorithm for inversion of electrical resistivity data is computationally efficient and can serve either as a stand-alone tool for layer delineation or as an autonomous module in a more comprehensive geophysical survey.

2. The inversion algorithm is most robust when each layer is sampled at least once. When one or more layers have not been sampled, the algorithm's robustness (convergence) depends on the accuracy of an initial guess (e.g., expert knowledge and other hard or soft data).

3. The presence of multiple layers can give rise to an objective function with multiple local and global minima. This necessitates the use of expanded searches.
4. Identification of regions with steep saturation gradients and multiple local minima can be used to design an efficient, cost-effective sampling strategy.

The present analysis is based on the following assumptions:

1. Archie's law and Gardner's model provide an adequate representation of the resistivity–saturation and conductivity–saturation relationships, respectively.
2. The number of layers comprising the vadose zone is known from geologic surveys, expert knowledge, or other soft data.
3. Each layer is macroscopically homogeneous.
4. The hydraulic and resistivity properties of each layer are known.

This problem formulation is clearly a simplification and serves as a starting point for future generalizations, in which one or more of the assumptions made above will be relaxed. While Archie's law (Eq. [1]) has a solid theoretical underpinning provided by percolation and effective-media theories (e.g., Hilfer, 1991; Ewing and Hunt, 2006), its applicability to many subsurface environments is questionable (e.g., Glover et al., 2000, and the references therein). Likewise, while the exponential model (Eq. [3]) often fails to provide the best fit to the data, it has been used extensively (see the literature review and the corresponding discussion in Lu et al., 2002). In future investigations, our approach will be extended to arbitrary constitutive laws by applying the analytical algorithm of Rockhold et al. (1997).

The assumptions that layers are homogeneous and that their parameters are known deterministically can be relaxed within a stochastic framework. One can either replace the spatially varying hydraulic parameters with their stochastically derived effective counterparts (e.g., Tartakovsky et al., 1999, 2003b, 2004; Lu et al., 2002) or provide a statistical description of soil properties by adopting the probabilistic approach of Neuman et al. (2007). Both approaches would use the solution developed in the present analysis as a leading-order approximation.

References

Binley, A., P. Winship, L.J. West, M. Pokar, and R. Middleton. 2002. Seasonal variation of moisture content in unsaturated sandstone inferred from borehole radar and resistivity profiles. J. Hydrol. 267:160–172.

Cornacchiulo, D., and A.C. Bagtzoglou. 2004. Geostatistical reconstruction of gaps in near-surface electrical resistivity data. Vadose Zone J. 3:1215–1229.

Dahlin, T. 1996. 2D resistivity surveying for environmental and engineering applications. First Break 14:275–283.

Dentz, M., and D.M. Tartakovsky. 2008. Self-consistent four-point closure for transport in steady random flows. Phys. Rev. E 77:066307, doi:10.1103/PhysRevE.77.066307.

Ewing, R.P., and A.G. Hunt. 2006. Dependence of the electrical conductivity on saturation in real porous media. Vadose Zone J. 5:731–741.

Furman, A., T.P.A. Ferré, and A.W. Warrick. 2004. Optimization of ERT surveys for monitoring transient hydrological events using perturbation sensitivity and genetic algorithms. Vadose Zone J. 3:1230–1239.

Glover, P.W.J., M.J. Hole, and J. Pous. 2000. A modified Archie's law for two conducting phases. Earth Planet. Sci. Lett. 180:369–383.

Griffiths, D.H., and R.D. Barker. 1993. Two-dimensional resistivity imaging and modeling in areas of complex geology. J. Appl. Geophys. 29:211–226.

Guadagnini, L., A. Guadagnini, and D.M. Tartakovsky. 2004. Probabilistic reconstruction of geologic facies. J. Hydrol. 294:57–67.

Hilfer, R. 1991. Geometric and dielectric characterization of porous media. Phys. Rev. B 44:60–75.

Hubbard, S.S., and Y. Rubin. 2000. Hydrogeological parameter estimation using geophysical data: A review of selected techniques. J. Contam. Hydrol. 45:3–34.

Kemna, A., B. Kulessa, and H. Vereecken. 2002. Imaging and characterisation of subsurface solute transport using electrical resistivity tomography (ERT) and equivalent transport models. J. Hydrol. 267:125–146.

Lagarias, J.C., J.A. Reeds, M.H. Wright, and P.E. Wright. 1998. Convergence properties of the Nelder–Mead simplex method in low dimensions. SIAM J. Optim. 9:112–147.

Liu, S., and T.-C.J. Yeh. 2004. An integrative approach for monitoring water movement in the vadose zone. Vadose Zone J. 3:681–692.

Lu, Z., S.P. Neuman, A. Guadagnini, and D.M. Tartakovsky. 2002. Conditional moment analysis of steady state unsaturated flow in bounded, randomly heterogeneous soils. Water Resour. Res. 38(4):1038, doi:10.1029/2001WR000278.

Michalak, A.M., and P.K. Kitanidis. 2003. A method for enforcing parameter nonnegativity in Bayesian inverse problems with an application to contaminant source identification. Water Resour. Res. 39(2):1033, doi:10.1029/2002WR001480.

Mundry, E., and H.-J. Zschau. 1983. Geoelectrical models involving layers with a linear change in resistivity and their use in the investigation of clay deposits. Geophys. Prospect. 31:810–828.

Nelder, J.A., and R. Mead. 1965. A simplex method for function minimization. Comput. J. 7:308–313.

Neuman, S.P. 1993. Eulerian–Lagrangian theory of transport in space–time nonstationary velocity fields: Exact nonlocal formalism by conditional moments and weak approximation. Water Resour. Res. 29:633–645.

Neuman, S.P., A. Blattstein, M. Riva, D.M. Tartakovsky, A. Guadagnini, and T. Ptak. 2007. Type curve interpretation of late-time pumping test data in randomly heterogeneous aquifers. Water Resour. Res. 43:W10421, doi:10.1029/2007WR005871.

Ritzi, R.W., D.F. Jayne, A.J. Zahradnik, A.A. Field, and G.E. Fogg. 1994. Geostatistical modeling of heterogeneity in glaciofluvial, buried-valley aquifers. Ground Water 32:666–674.

Rockhold, M.L., C.S. Simmons, and M.J. Fayer. 1997. An analytical solution technique for one-dimensional, steady vertical water flow in layered soils. Water Resour. Res. 33:897–902.

Rubin, Y. 2003. Applied stochastic hydrogeology. Oxford Univ. Press, New York.

Sato, H.K. 2000. Potential field from a dc current source arbitrarily located in a nonuniform layered medium. Geophysics 65:1726–1732.

Sato, H.K., and E.S. Sampaio. 1980. Electrical sounding of a half-space with a monotonic continuous variation of the resistivity with depth. Geophys. Prospect. 28:967–976.

Spies, B.R. 1996. Electrical and electromagnetic borehole measurements: A review. Surv. Geophys. 17:517–556.

Storz, H., W. Storz, and F. Jacobs. 2000. Electrical resistivity tomography to investigate geological structure of the earth's upper crust. Geophys. Prospect. 48:455–471.

Tartakovsky, A.M., L. Garcia-Naranjo, and D.M. Tartakovsky. 2004. Transient flow in a heterogeneous vadose zone with uncertain parameters. Vadose Zone J. 3:154–163.

Tartakovsky, D.M., and A. Guadagnini. 2001. Prior mapping for nonlinear flows in random environments. Phys. Rev. E 64:5302(R)–5305(R).

Tartakovsky, D.M., A. Guadagnini, and M. Riva. 2003. Stochastic averaging of nonlinear flows in heterogeneous porous media. J. Fluid Mech. 492:47–62.

Tartakovsky, D.M., Z. Lu, A. Guadagnini, and A.M. Tartakovsky. 2003b. Unsaturated flow in heterogeneous soils with spatially distributed uncertain hydraulic parameters. J. Hydrol. 275:182–193.

Tartakovsky, D.M., S.P. Neuman, and Z. Lu. 1999. Conditional stochastic averaging of steady state unsaturated flow by means of Kirchhoff transformation. Water Resour. Res. 35:731–745.

Tartakovsky, D.M., and C.L. Winter. 2008. Uncertain future of hydrogeology. J. Hydrol. Eng. 13:37–39.

Tartakovsky, D.M., B.E. Wohlberg, and A. Guadagnini. 2007. Nearest neighbor classification for facies delineation. Water Resour. Res. 43:W07201,

doi:10.1029/2007WR005968.

Vereecken, H., S. Hubbard, A. Binley, and T. Ferré. 2004. Hydrogeophysics: An introduction by the guest editors. Vadose Zone J. 3:1060–1062.

Winter, C.L., and D.M. Tartakovsky. 2000. Mean flow in composite porous media. Geophys. Res. Lett. 27:1759–1762.

Winter, C.L., and D.M. Tartakovsky. 2002. Groundwater flow in heterogeneous composite aquifers. Water Resour. Res. 38(8):1148, doi:10.1029/2001WR000450.

Winter, C.L., D.M. Tartakovsky, and A. Guadagnini. 2002. Numerical solutions of moment equations for flow in heterogeneous composite aquifers. Water Resour. Res. 38(5):1055, doi:10.1029/2001WR000222.

Wohlberg, B.E., D.M. Tartakovsky, and A. Guadagnini. 2006. Subsurface characterization with support vector machines. IEEE Trans. Geosci. Remote Sens. 44:47–57.

Yeh, T.-C.J., S. Liu, R.J. Glass, K. Baker, J.R. Brainard, D.L. Alumbaugh, and D. LaBrecque. 2002. A geostatistically based inverse model for electrical resistivity surveys and its applications to vadose zone hydrology. Water Resour. Res. 38(12):1278, doi:10.1029/2001WR001204.